


 Cite this: *RSC Adv.*, 2020, **10**, 16045

 Received 22nd February 2020
 Accepted 7th April 2020

 DOI: 10.1039/d0ra01703e
rsc.li/rsc-advances

A one-dimensional infinite silver alkynyl assembly $[\text{Ag}_8(\text{C}\equiv\text{C}^t\text{Bu})_5(\text{CF}_3\text{COO})_3(\text{CH}_3\text{CN})]_n$: synthesis, crystal structure and properties†

Ju-Feng Shi, Zhi-Jin Chen, Liu-Jie Zhang, Kun Zhou, * Jiu-Yu Ji and Yan-Feng Bi *

A high-yield silver alkynyl assembly $[\text{Ag}_8(\text{C}\equiv\text{C}^t\text{Bu})_5(\text{CF}_3\text{COO})_3(\text{CH}_3\text{CN})]_n$ (**1**) constructed from $[\text{AgC}\equiv\text{C}^t\text{Bu}]_n$ ligand, CF_3COOAg and CH_3CN auxiliary ligands with a one-dimensional infinite chain structure has been obtained in one pot. Compound **1** has been well-defined and characterized. The photocurrent properties and the temperature-sensitive luminescent properties of **1** have been investigated.

Nano-structured architectures, as a rapidly developing and widely accepted new functional material, have potential applications, such as in bioelectronics, sensing and catalysis.¹ Transition metal clusters with precise atomic composition are a kind of nanoscale material. For example, coinage metal (copper, silver, gold) clusters have widely attracted attention from more and more chemists owing to their extremely fascinating structures and rich physicochemical properties.² Among these, high-nuclearity silver clusters have received researchers' attention for a long time mainly due to the excellent coordination mode of silver for ligands and their promising applications.^{3,4} Meanwhile inorganic synthesis technology is becoming mature, the synthesis of large inorganic clusters and so-called cluster compounds at the nanoscale has a wide variety of novel structures. However, it involves a complicated process to prepare high-nuclearity silver clusters.⁵ Many factors can affect the formation of clusters, so it is difficult to predict their final structures and control their compositions. At present, most of the studies are still at the structural level and there are only a few further explorations of their properties.⁶

$\text{RC}\equiv\text{C}$ and S-, P-, N-R (R = alkyl) are important organic ligands in silver cluster compounds. Silver acetylides, as one of typical silver clusters, with structure diversity and charming properties⁷ have also been widely studied. A great many multi-nuclear silver alkynyl compounds constructed by a basic comonomer or aggregate $[\text{AgC}\equiv\text{CR}]_n$ have been reported so far. It is considerably untoward that $[\text{AgC}\equiv\text{CR}]_n$ is insoluble and the solution can be dissolved by adding some soluble silver salts.⁸ Although a significant advantage of alkynyl ligands over other

organic ligands containing S, P or N atom is its $\text{C}\equiv\text{C}$ bond, which can attach to a metal surface by forming both σ and π bonds.³ Therefore alkynyl ligands as electron acceptors tend to build cluster compounds by $\text{p}\pi\text{-d}\pi$ conjugation with metal.⁹ For instance, spectroscopic and crystallographic data fully demonstrate that the arsenic-based ligand $\text{RC}\equiv\text{C}$ terminal exhibits a versatile coordination mode, good σ -donor and weak acceptor characteristics towards transition metals during the formation of various compounds.¹⁰ Another common problem in the silver alkynyl system is that the yield of silver clusters is generally not high, which limits further research on their properties. Above all, control synthesis of high-yield higher nuclearity clusters, multinuclear aggregates and even extended solid-state architectures involving the ethynide moiety with diverse coordination modes and metal silver centers consolidated by metallophilic interactions is our ultimate goal.¹¹

Based on what we have discussed above, a continuous investigation into the silver alkynyl compounds is going in our group.¹² A high-yield alkynyl silver compound $[\text{Ag}_8(\text{C}\equiv\text{C}^t\text{Bu})_5(\text{CF}_3\text{COO})_3(\text{CH}_3\text{CN})]$ (**1**) was obtained by the assembly of $[\text{AgC}\equiv\text{C}^t\text{Bu}]_n$ and CF_3COOAg in a molar ratio of 1 : 1 in the acetonitrile. Compound **1** has been well-defined and characterized. And the UV-vis solid-state optical diffuse reflectance spectrum, the band gap and the photocurrent property of **1** have been investigated. In addition, the temperature-sensitive luminescent property of **1** has also been studied, in which the maximum emission intensity and the temperature present an excellent linear relationship.

Firstly, $[\text{AgC}\equiv\text{C}^t\text{Bu}]_n$ and CF_3COOAg in a molar ratio of 1 : 1 are dissolved in the acetonitrile, which is transferred into a Teflon-lined stainless autoclave and kept at 70 °C for 24 h. Then the suspension is naturally cooled to room temperature and is filtered. Lastly, the colorless block crystals **1** (yield: ca. 53% based on Ag) are precipitated from the filtrate two days later. The crystal structure of compound

School of Chemistry and Materials Science, Liaoning Shihua University, Fushun, Liaoning 113001, China. E-mail: zhouk800@aliyun.com; biyanfeng@lnpu.edu.cn

† Electronic supplementary information (ESI) available: Synthetic procedures, crystallographic studies and physical measurements. CCDC 1978916. For ESI and crystallographic data in CIF or other electronic format see DOI: 10.1039/d0ra01703e



$[\text{Ag}_8(\text{C}\equiv\text{C}'\text{Bu})_5(\text{CF}_3\text{COO})_3(\text{CH}_3\text{CN})]_n$ (**1**) was explicitly analyzed by single crystal X-ray diffraction and the result reveals that the space group of compound **1** crystallized in the triclinic P-1. The whole configuration of this crystal can be described as a one-dimensional infinite chain. In an asymmetric unit, it contains eight silver atoms, five $\text{Bu}'\text{C}\equiv\text{C}^-$ ligands, three CF_3COO^- ligands and one CH_3CN ligand, as shown in Fig. 1. It shows that the eight silver atoms displayed in the center construct the primary skeleton, while the $\text{Bu}'\text{C}\equiv\text{C}^-$, CF_3COO^- as well as CN^- ligands in the periphery can commendably support the framework of the $\text{Ag}_8(\text{C}\equiv\text{C}'\text{Bu})_5(\text{CF}_3\text{COO})_3(\text{CH}_3\text{CN})$ unit. In detail, the five $\text{Bu}'\text{C}\equiv\text{C}^-$ ligands separately adopting the four different geometric coordination modes, $\mu_4\text{-}\eta^3\text{:}\eta^3\text{:}\eta^3\text{:}\eta^4$ ($\text{C}1\equiv\text{C}2$, $\text{C}13\equiv\text{C}14$), $\mu_3\text{-}\eta^3\text{:}\eta^3\text{:}\eta^3$ ($\text{C}7\equiv\text{C}8$) and $\mu_3\text{-}\eta^2\text{:}\eta^3\text{:}\eta^4$ ($\text{C}19\equiv\text{C}20$, $\text{C}25\equiv\text{C}26$) are tied to the eight silver(i) ions to construct the $[\text{Ag}_8(\text{C}\equiv\text{C}'\text{Bu})_5]^{3+}$ framework, which is further consolidated by the three CF_3COO^- ligands in the $\mu_2\text{-O}$, O' ($\text{O}1\text{-O}2$ and $\text{O}3\text{-O}4$) and $\mu_3\text{-O}$, O' ($\text{O}7\text{-O}8$) modes as well as the one monodentate CH_3CN ligand. Such two asymmetric units can be fused into a dimer through the $\text{Ag}\cdots\text{Ag}$ interactions in the range of $2.9232(6)\text{-}3.2117(5)$ Å between the two components, as shown in Fig. 2. Therefore, the integrated silver skeleton of **1** can be seen in Fig. 2. It is clearly that the sixteen silver atoms can form silver triangles and quadrangles through the $\text{Ag}\cdots\text{Ag}$ interactions.¹³

In an asymmetric unit of compound **1**, the eight silver atoms can be anatomically segmented into the three types, η^2 , η^3 and η^4 . The $\text{Ag}7$ atom adopting the first η^2 mode was bonded to a pair of opposite $\text{C}19\equiv\text{C}20$ and $\text{C}25\equiv\text{C}26$ alkynyl ligands in the $\mu_3\text{-}\eta^2\text{:}\eta^3\text{:}\eta^4$ with the Ag-C bond distance $2.072(4)$ and $2.098(4)$ Å. The second η^3 mode covers five silver atoms ($\text{Ag}2$, $\text{Ag}3$, $\text{Ag}4$, $\text{Ag}5$ and $\text{Ag}8$), which joint one oxygen atom, one or two carbons, and another nitrogen atom separately from CF_3COO^- ligands with the Ag-O bond distance $2.300(3)\text{-}2.517(3)$ Å, $\text{Bu}'\text{C}\equiv\text{C}^-$ ligands with Ag-C bond distance $2.134(4)\text{-}2.629(4)$ Å and CH_3CN ligand with Ag-N bond distance $2.239(5)$ Å. The third kind contains two $\text{Ag}1$ and $\text{Ag}6$ atoms in the η^4 mode link the oxygen atoms from CF_3COO^- ligand (Ag-O $2.288(3)\text{-}2.443(3)$ Å) and the carbon atoms from $\text{Bu}'\text{C}\equiv\text{C}^-$ ligands (Ag-C $2.368(4)\text{-}2.532(4)$ Å).

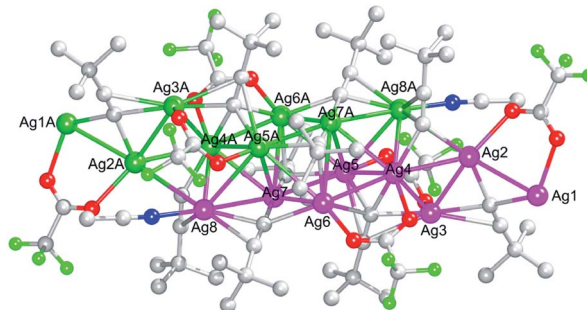


Fig. 2 The standard ball and stick model of a dimer constructed by the two $\text{Ag}_8(\text{Bu}'\text{C}\equiv\text{C})_5(\text{CF}_3\text{COO})_3(\text{CH}_3\text{CN})$ asymmetric unit of **1**. For the sake of clarity, all hydrogen atoms are omitted. Color code: Ag, pink; C, gray-50%; N, blue; O, red; F, bright green.

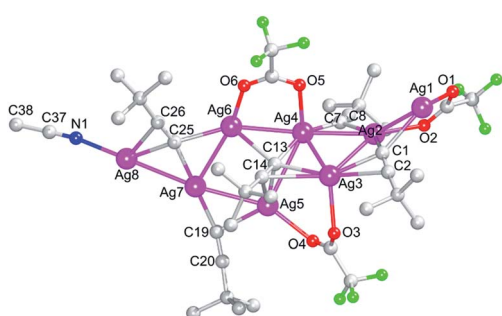


Fig. 1 The standard ball and stick model of the $\text{Ag}_8(\text{Bu}'\text{C}\equiv\text{C})_5(\text{CF}_3\text{COO})_3(\text{CH}_3\text{CN})$ asymmetric unit of **1**. For the sake of clarity, all hydrogen atoms are omitted. Color code: Ag, pink; C, gray-50%; N, blue; O, red; F, bright green.

And a one-dimensional infinite chain is constructed by the adjacent $\text{Ag}_8(\text{C}\equiv\text{C}'\text{Bu})_5(\text{CF}_3\text{COO})_3(\text{CH}_3\text{CN})$ dimers depending on the $\text{Ag}1\text{-O}5\#1$, $\text{Ag}1\text{-C}1\#1$, $\text{Ag}1\#1\text{-O}5$, $\text{Ag}1\#1\text{-C}1$ bonds with the Ag-O bond length $2.443(3)$ Å and the Ag-C bond length $2.428(4)$ Å together with the $\text{Ag}1\cdots\text{Ag}1\#1$, $\text{Ag}1\cdots\text{Ag}2\#1$, $\text{Ag}1\cdots\text{Ag}3\#1$, $\text{Ag}1\#1\cdots\text{Ag}2$, $\text{Ag}1\#1\cdots\text{Ag}3$ interactions in the range of $2.9232(6)\text{-}3.1730(5)$ Å (<3.44 Å),¹⁴ as shown in Fig. 3.

By comparing the powder X-ray diffraction patterns (PXRDs) under experimental and simulated conditions, it can be proved whether the product is pure phase and can provide a basis for other subsequent tests. As shown in Fig. S1,[†] we can see that the experimental PXRD is consistent with the curves of the simulated PXRD. Hence, the phase purity of **1** can be clearly confirmed. Infrared spectrum (IR) can show the absorption of characteristic functional groups, so the composition of compound **1** was confirmed by IR data. As shown in Fig. S2,[†] the IR band at 3448 cm^{-1} is due to the O-H vibration, the band at 2968 cm^{-1} is due to the C-H vibration, the band at 2220 cm^{-1} is attributed to the $\text{C}\equiv\text{N}$ vibration, the band at 2017 cm^{-1} is attributed to the $\text{C}\equiv\text{C}$ vibration. The stretching vibration of C=O at 1675 cm^{-1} and C-F at 1208 cm^{-1} can prove the existence of CF_3COO^- . The thermogravimetric analysis (TGA) shows that the weight loss of compound **1** can be mainly divided into two parts, as depicted in Fig. S3.[†] The first step of weight loss before $85\text{ }^\circ\text{C}$ may be caused by the loss of acetonitrile solvent attached to the crystal. The second step of weight loss before $310\text{ }^\circ\text{C}$ should be due to the shedding of the peripheral CH_3CN , CF_3COO^- and $\text{Bu}'\text{C}\equiv\text{C}^-$ ligands. When temperature is higher than $310\text{ }^\circ\text{C}$, the compound starts to decompose. Until after $530\text{ }^\circ\text{C}$, the thermogravimetric ratio of **1** basically remains unchanged.

The UV-vis solid-state optical diffuse reflectance spectrum was measured at room temperature, as shown in Fig. 4. It is clearly that compound **1** exhibits a broad absorption peak at 268 nm in the ultraviolet region, which should be assigned to the $\pi\text{-}\pi^*$ transition of the $\text{Bu}'\text{C}\equiv\text{C}^-$ ligands in **1**.¹⁵ Furthermore, the band gap of **1** was estimated to be 2.56 eV . Thus compound **1** is a potential semiconductor material.

In order to study the photoelectrochemical property of compound **1**, the photocurrent response curves ($i\text{-}t$ curves) were



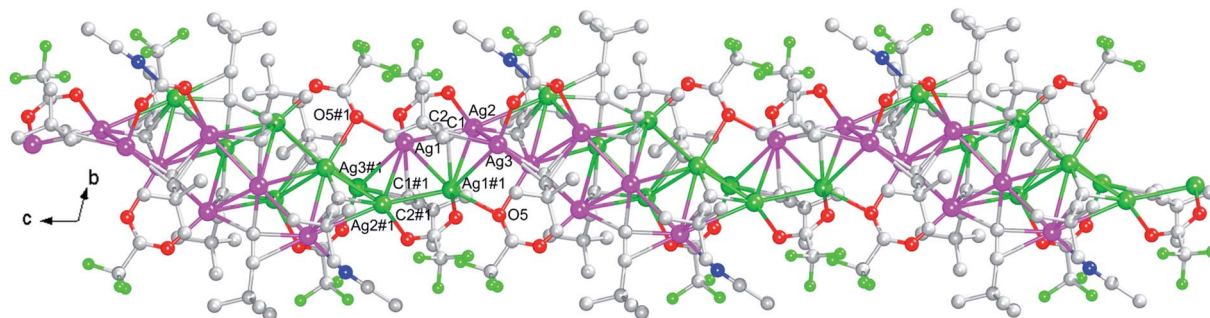


Fig. 3 The one-dimensional chain of **1**. For the sake of clarity, all hydrogen atoms are omitted. Color code: Ag, pink and green; C, gray-50%; N, blue; O, red; F, bright green.

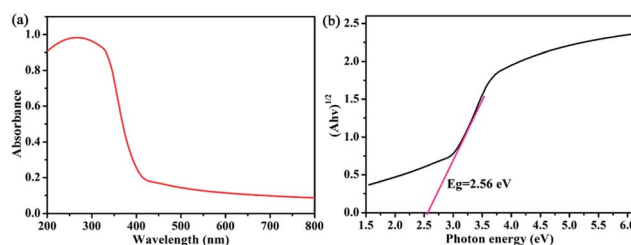


Fig. 4 (a) The UV-vis solid-state optical diffuse reflectance spectrum of **1**. (b) The band gap of **1**.

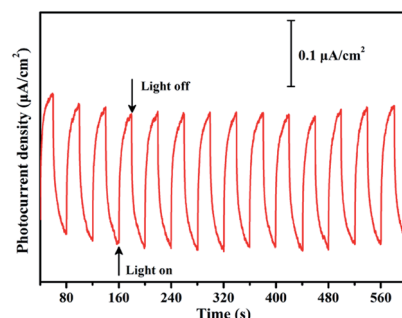


Fig. 5 Photocurrent response of **1** under repeated irradiation in 0.2 M Na₂SO₄ aqueous solution.

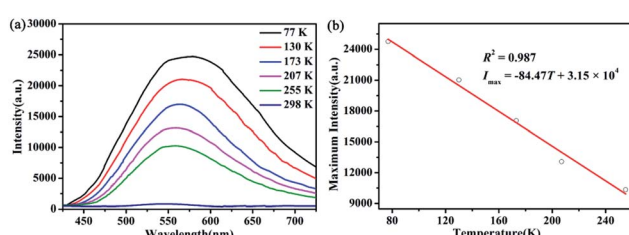


Fig. 6 (a) Luminescent spectra of **1** recorded in the solid state from 298 to 77 K under the excitation of 396 nm. (b) Linear relationship between maximum emission intensity and temperature of **1**.

measured at a fixed bias potential of 1.23 V vs. RHE *via* on-off cycles of irradiation. As shown in Fig. 5, the rise and fall of the photocurrents corresponded well to the switching on and off of

the irradiation. When the irradiation was interrupted, the photocurrent exhibited a prominent decline, and the photocurrent reverted to the original value once light was switched on again. At the bias of 1.23 V vs. RHE, the photocurrent density of compound **1** is nearly 0.2 $\mu\text{A cm}^{-2}$. The photocurrent density has no obvious decline after 14 on/off cycles, indicating the photoelectrode possesses excellent photochemical stability.¹⁶ The mechanism of photocurrent generation is proposed as follow. Upon illumination, the electrons in the valence band (VB) (predominately 2p-C) of compound **1** are excited to its conduction band (CB) (mainly 5s-Ag),^{2a} then the opposite transmission of photogenerated electron and hole produces photocurrent. Thus compound **1** should have potential applications in photoelectrochemistry.

The photoluminescence properties of solid compound **1** have been studied.¹⁷ According to Fig. 6a, compound **1** has a good emission behavior at an excitation wavelength of 396 nm at different temperature from 298 K, 255 K, 207 K, 173 K, 130 K to 77 K. Obviously, its emission intensity is correspondingly increased as the temperature is gradually reduced from 298 K to 77 K. It is because the rigidity of compound **1** is enhanced and the system span of heavy metals is reduced as the temperature decreases. In addition, transfer of ligand to metal transfer (LMCT) is caused by energy loss from non-radiative decay and enhancement of Ag…Ag interaction.¹⁸ At 298 K, the maximum emission wavelength of **1** is 545 nm. As the temperature decreases from 298 to 77 K, the maximum emission wavelength shifts slightly to 578 nm.¹⁹ It has a good linear relationship between the maximum emission intensity of **1** and the corresponding temperature from 77 K to 298 K, as shown in Fig. 6b. The linear equation is $I_{\text{max}} = -84.47T + 3.15 \times 10^4$ and the correlation coefficient is 0.993.^{2a} The results indicate that compound **1** will be a potential temperature-sensitive probe.

Conclusions

In summary, it provides a simple method to prepare a high-yield one-dimensional infinite silver alkynyl chain $[\text{Ag}_8(\text{C}\equiv\text{C}'\text{Bu})_5(\text{CF}_3\text{COO})_3(\text{CH}_3\text{CN})]_n$ (**1**) by the assembly of $[\text{AgC}\equiv\text{C}'\text{Bu}]_n$ ligand, CF₃COOAg and CH₃CN auxiliary ligands through solvothermal method. Through our research towards its synthesis, structure and property, compound **1** has been proved to be a potential



semiconductor material, photoelectrochemical material and temperature-sensitive probe. Further studies on silver alkynyl clusters are under way in our group.

Conflicts of interest

There are no conflicts to declare.

Acknowledgements

This work was supported by Talent Scientific Research Fund of LSHU (No. 2016XJJ-011), Scientific Research Cultivation Fund of LSHU (No. 2016PY-015), Education Department of Liaoning Province Basic Research Project (No. L2017LQN009 and L2017LQN029), and the National Natural Science Foundation of China (No. 91961110).

Notes and references

- (a) F. Gruber and M. Jansen, *Z. Anorg. Allg. Chem.*, 2011, **637**, 1676–1679; (b) Y.-Y. Liu, X.-Q. Chai, M.-Y. Chen, R.-C. Jin, W.-P. Ding and Y. Zhu, *Angew. Chem., Int. Ed.*, 2018, **57**, 9775–9779; (c) G.-X. Duan, L. Tian, J.-B. Wen, L.-Y. Li, Y.-P. Xie and X. Lu, *Nanoscale*, 2018, **10**, 18915–18919; (d) J. Chai, S. Yang, Y. Lv, T. Chen, S. Wang, H. Yu and M.-Z. Zhu, *J. Am. Chem. Soc.*, 2018, **140**, 15582–15585; (e) S.-F. Yuan, Z.-J. Guan, W.-D. Liu and Q.-M. Wang, *Nat. Commun.*, 2019, **10**, 4032.
- (a) S.-S. Zhang, H.-F. Su, G.-L. Zhuang, X.-P. Wang, C.-H. Tung, D. Sun and L.-S. Zheng, *Chem. Commun.*, 2018, **54**, 11905–11908; (b) Y.-P. Xie, J.-L. Jin, G.-X. Duan, X. Lu and T. C. W. Mak, *Coord. Chem. Rev.*, 2017, **331**, 54–72; (c) R. C. Jin, C. J. Zeng, M. Zhou and Y. X. Chen, *Chem. Rev.*, 2016, **116**, 10346–10413; (d) Z. Wang, H.-F. Su, Y.-Z. Tan, S. Schein, S.-C. Lin, W. Liu, S.-A. Wang, W.-G. Wang, C.-H. Tung, D. Sun and L.-S. Zheng, *Proc. Natl. Acad. Sci. U. S. A.*, 2017, **114**, 12132–12137; (e) Y. L. Li, Z. Y. Wang, X. H. Ma, P. Luo, C. X. Du and S. Q. Zang, *Nanoscale*, 2019, **11**, 5151–5157.
- (a) Z. Lei, X.-K. Wan, S.-F. Yuan, Z.-J. Guan and Q.-M. Wang, *Acc. Chem. Res.*, 2018, **51**, 2465–2474; (b) X.-Y. Dong, H.-L. Huang, J.-Y. Wang, H.-Y. Li and S.-Q. Zang, *Chem. Mater.*, 2018, **30**, 2160–2167; (c) S. Li, X.-S. Du, B. Li, J.-Y. Wang, G.-P. Li, G.-G. Gao and S.-Q. Zang, *J. Am. Chem. Soc.*, 2018, **140**, 594–597; (d) Z.-Y. Wang, M.-Q. Wang, Y.-L. Li, P. Luo, T.-T. Jia, W. R. Huang, S.-Q. Zang and T. C. W. Mak, *J. Am. Chem. Soc.*, 2018, **140**, 1069–1076; (e) Z. Han, X.-Y. Dong, P. Luo, S. Li, Z.-Y. Wang, S.-Q. Zang and T. C. W. Mak, *Sci. Adv.*, 2020, **6**, eaay0107.
- (a) S. Sharma, K. K. Chakrabarti, J.-Y. Saillard and C. W. Liu, *Acc. Chem. Res.*, 2018, **51**, 2475–2483; (b) Q.-F. Yao, T.-K. Chen, X. Yuan and J.-P. Xie, *Acc. Chem. Res.*, 2018, **51**, 1338–1348; (c) Q.-M. Wang, Y.-M. Lin and K.-G. Liu, *Acc. Chem. Res.*, 2015, **48**, 1570–1579; (d) X. Kang and M.-Z. Zhu, *Coord. Chem. Rev.*, 2019, **394**, 1–38; (e) H.-Y. Yang, J.-Z. Yan, Y. Wang, H.-F. Su, L. Gell, X.-J. Zhao, C.-F. Xu, B. K. Teo, H. Häkkinen and N.-F. Zheng, *J. Am. Chem. Soc.*, 2017, **139**, 31–34; (f) O. Fuhr, S. Dehnen and D. Fenske, *Chem. Soc. Rev.*, 2013, **42**, 1871–1906.
- (a) Z. Wang, H.-F. Su, M. Kurmoo, C.-H. Tung, D. Sun and L.-S. Zheng, *Nat. Chem.*, 2018, **9**, 2094; (b) Y. Wang, X.-K. Wan, L. Ren, H.-F. Su, G. Li, S. Malola, S.-C. Lin, Z.-C. Tang, H. Häkkinen, B. K. Teo, Q.-M. Wang and N.-F. Zheng, *J. Am. Chem. Soc.*, 2016, **138**, 3278–3281; (c) J. N. Anker, W. P. Hall, O. Lyandres, N. C. Shah, J. Zhao and R. P. V. Duyne, *Nat. Mater.*, 2008, **7**, 442–453; (d) R.-C. Jin, Y.-C. Cao, E. Hao, G. S. Métraux, G. C. Schatz and C. A. Mirkin, *Nature*, 2003, **425**, 487–490; (e) Z. Wang, H.-F. Su, C.-H. Tung, D. Sun and L.-S. Zheng, *Nat. Chem.*, 2018, **9**, 4407–4414.
- (a) Y. Yang, S.-S. Zhang, Q.-Q. Zhao, X.-P. Wang, C.-H. Tung and D. Sun, *Eur. J. Inorg. Chem.*, 2018, 5068–5074; (b) U. Halbes-Letinois, J.-M. Weibel and P. Pale, *Chem. Soc. Rev.*, 2007, **36**, 759–769; (c) V. W.-W. Yam, V. K.-M. Au and S. Y.-L. Leung, *Chem. Rev.*, 2015, **115**, 7589–7728; (d) K. A. Green, M. P. Cifuentes, M. Samoc and M. G. Humphrey, *Coord. Chem. Rev.*, 2011, **255**, 2530–2541.
- (a) M. Cao, R. Pang, Q.-Y. Wang, Z. Han, Z.-Y. Wang, X.-Y. Dong, S.-F. Li, S.-Q. Zang and T. C. W. Mak, *J. Am. Chem. Soc.*, 2019, **141**, 14505–14509; (b) S.-S. Zhang, F. Alkan, H.-F. Su, C. M. Aikens, C. H. Tung and D. Sun, *J. Am. Chem. Soc.*, 2019, **141**, 4460–4467; (c) X. Kang, X. Wei, S. Jin, Q.-Q. Yuan, X.-Q. Luan, Y. Pei, S.-X. Wang, M.-Z. Zhu and R.-C. Jin, *Proc. Natl. Acad. Sci. U. S. A.*, 2019, **116**, 18834–18840; (d) S. Li, Z.-Y. Wang, G.-G. Gao, B. Li, P. Luo, Y.-J. Kong, H. Liu and S.-Q. Zang, *Angew. Chem., Int. Ed.*, 2018, **57**, 12775–12779; (e) Y.-M. Su, H.-F. Su, Z. Wang, Y.-A. Li, S. Schein, Q.-Q. Zhao, X.-P. Wang, C. H. Tung, D. Sun and L.-S. Zheng, *Chem. - Eur. J.*, 2018, **24**, 15096–15103.
- (a) Q.-M. Wang and T. C. W. Mak, *J. Am. Chem. Soc.*, 2000, **122**, 7608–7609; (b) M.-L. Chen, X.-F. Xu, Z.-X. Cao and Q.-M. Wang, *Inorg. Chem.*, 2008, **47**, 1877–1879.
- (a) L. Zhao, C.-Q. Wan, J. Han, X.-D. Chen and T. C. W. Mak, *Chem. - Eur. J.*, 2008, **14**, 10437–10444; (b) Z.-G. Jiang, K. Shi, Y.-M. Lin and Q.-M. Wang, *Chem. Commun.*, 2014, **50**, 2353–2355.
- (a) J. Forniés, S. Fuertes, A. Martín, V. Sicilia, E. Lalinde and M. T. Moreno, *Chem. - Eur. J.*, 2006, **12**, 8253–8266; (b) A. B. Antonova, M. I. Bruce, P. A. Humphrey, M. Gaudio, B. K. Nicholson, N. Scoleri, B. W. Skelton, A. H. White and N. N. Zaitseva, *J. Organomet. Chem.*, 2006, **691**, 4694–4707; (c) C. W. Baxter, T. C. Higgs, P. J. Bailey, S. Parsons, F. McLachlan, M. McPartlin and P. A. Tasker, *Chem. - Eur. J.*, 2006, **12**, 6166–6174.
- (a) L. Zhao, W.-Y. Wong and T. C. W. Mak, *Chem. - Eur. J.*, 2006, **12**, 4865–4872; (b) X. Kang and M. Z. Zhu, *Chem. Soc. Rev.*, 2019, **48**, 2422–2457.
- (a) A. Xie, Z. Wang, L.-P. Cheng, G.-G. Luo, Q.-Y. Liu and D. Sun, *Eur. J. Inorg. Chem.*, 2019, 496–501; (b) J.-W. Liu, H.-F. Su, Z. Wang, Y.-A. Li, Q.-Q. Zhao, X.-P. Wang, C.-H. Tung, D. Sun and L.-S. Zheng, *Chem. Commun.*, 2018, **54**, 4461–4464; (c) J.-W. Liu, L. Feng, H.-F. Su, Z. Wang, Q.-Q. Zhao, X.-P. Wang, C.-Ho Tung, D. Sun and L.-S. Zheng, *J. Am. Chem. Soc.*, 2018, **140**, 1600–1603; (d)



S. Jin, S.-X. Wang, Y.-B. Song, M. Zhou, J. Zhong, J. Zhang, A.-D. Xia, Y. Pei, M. Chen, P. Li and M.-Z. Zhu, *J. Am. Chem. Soc.*, 2014, **136**, 15559–15565.

13 (a) Y. Yang, T. Jia, Y.-Z. Han, Z.-A. Nan, S.-F. Yuan, F.-L. Yang and D. Sun, *Angew. Chem., Int. Ed.*, 2019, **58**, 12280–12285; (b) Z.-J. Guan, F. Hu, S.-F. Yuan, Z.-A. Nan, Y.-M. Lin and Q.-M. Wang, *Chem. Sci.*, 2019, **10**, 3360–3365; (c) J.-Y. Liu, F. Alkan, Z. Wang, Z.-Y. Zhang, M. Kurmoo, Z. Yan, Q.-Q. Zhao, C. M. Aikens, C.-H. Tung and D. Sun, *Angew. Chem., Int. Ed.*, 2019, **58**, 195–199; (d) J.-L. Jin, Y.-P. Xie, H. Cui, G.-X. Duan, X. Lu and T. C. W. Mak, *Inorg. Chem.*, 2017, **56**, 10412–10417; (e) W.-T. Chang, P.-Y. Lee, J.-H. Liao, K. K. Chakrabarti, S. Kahlal, Y.-C. Liu, M.-H. Chiang, J.-Y. Saillard and C. W. Liu, *Angew. Chem., Int. Ed.*, 2017, **56**, 10178–10182.

14 A. Bondi, *J. Phys. Chem.*, 1964, **68**, 441–451.

15 J.-W. Liu, Z. Wang, Y.-M. Chai, M. Kurmoo, Q.-Q. Zhao, X.-P. Wang, C. H. Tung and D. Sun, *Angew. Chem., Int. Ed.*, 2019, **58**, 6276–6279.

16 (a) Z. Wang, H.-F. Su, Y.-W. Gong, Q.-P. Qu, Y.-F. Bi, C.-H. Tung, D. Sun and L.-S. Zheng, *Nat. Commun.*, 2020, **308**, 594; (b) K. Sheng, L.-M. Fan, X.-F. Tian, R. K. Gupta, L.-N. Gao, C.-H. Tung and D. Sun, *Sci. China: Chem.*, 2020, **63**, 182–186.

17 (a) P.-P. Sun, Z. Wang, Y.-T. Bi, D. Sun, T. Zhao, F.-F. Zhao, W.-S. Wang and X. Xin, *ACS Appl. Nano Mater.*, 2020, **3**, 2038–2046; (b) Z.-J. Guan, J.-L. Zeng, S.-F. Yuan, F. Hu, Y.-M. Lin and Q.-M. Wang, *Angew. Chem., Int. Ed.*, 2018, **57**, 5703–5707; (c) G.-C. Liu, Y. Li, J. Chi, N. Xu, X.-L. Wang, H.-Y. Lin and Y.-Q. Chen, *Dyes Pigm.*, 2020, **174**, 108064; (d) Z.-C. Xie, P.-P. Sun, Z. Wang, H.-G. Li, L.-Y. Yu, D. Sun, M.-J. Chen, Y.-T. Bi, X. Xin and J.-C. Hao, *Angew. Chem., Int. Ed.*, 2019, DOI: 10.1002/anie.201912201.

18 (a) R.-W. Huang, X.-Y. Dong, B.-J. Yan, X.-S. Du, D.-H. Wei, S.-Q. Zang and T. C. W. Mak, *Angew. Chem., Int. Ed.*, 2018, **57**, 8560–8566; (b) Z. Wang, J.-W. Liu, H.-F. Su, Q.-Q. Zhao, M. Kurmoo, X.-P. Wang, C.-H. Tung, D. Sun and L. S. Zheng, *J. Am. Chem. Soc.*, 2019, **141**, 17884–17890.

19 (a) Z. Wang, H.-T. Sun, M. Kurmoo, Q.-Y. Liu, G.-L. Zhuang, Q.-Q. Zhao, X.-P. Wang, C.-H. Tung and D. Sun, *Chem. Sci.*, 2019, **10**, 4862–4867; (b) Y.-M. Su, Z. Wang, G.-L. Zhuang, Q.-Q. Zhao, X.-P. Wang, C.-H. Tung and D. Sun, *Chem. Sci.*, 2019, **10**, 564–568; (c) C. Liu, T. Li, H. Abroshan, Z.-M. Li, C. Zhang, H. J. Kim, G. Li and R.-C. Jin, *Nat. Commun.*, 2018, **9**, 744; (d) R.-W. Huang, Y.-S. Wei, X.-Y. Dong, X.-H. Wu, C.-X. Du, S.-Q. Zang and T. C. W. Mak, *Nat. Chem.*, 2017, **9**, 689–697.

